Supplemental Information:

Measurement of sub-4 nm particle emission from FFF-3D printing with the TSI Nano Enhancer and the Airmodus Particle Size Magnifier

Chi-Long Tang[a], Stefan Seeger[b]

[a]Materials and the Environment, Federal Institute for Materials Research and Testing (BAM), Berlin, Germany

[b]Analytical Chemistry; Reference Materials, Federal Institute for Materials Research and Testing (BAM), Berlin, Germany

CONTACT Chi-Long Tang chi-long.tang@bam.de Materials and the Environment, Federal Institute for Materials Research and Testing (BAM), Unter den Eichen 87, 12205 Berlin, Germany.

Table of Contents

Figures:

Tables:

Calibration data und data inversion calculations for the A11 nCNC

Table S1: Saturator flow rate and the corresponding D_{50} as calibrated by the manufacturer

Saturator flow rate [L/min]	D_{50} [nm]
0.096	4
0.113	3.02
0.133	2.69
0.156	2.3
0.184	2.04
0.255	1.93
0.3	1.87
0.353	1.79
0.416	1.7
0.576	1.59
0.678	1.55
0.797	1.5
1.3	1.38

The measured total particle number concentration, N, was corrected with the dilution factor of 5.5 according to equation 1.

$$N^* = N \cdot 5.5 \qquad \text{(Equation 1)}$$

For the determination of the particle number size distributions (PNSD) the existing good repeatability of the emission was a prerequisite. Firstly, TPNC($D_{50,i}$) measurements under exactly same conditions but with different cut-off diameters ($D_{50,i}$) from Table S1 were performed. Secondly, the normalized PNSD were calculated using Equation 2-4. Here, dN^* designates the absolute difference between two TPNC time series with adjacent cut-off diameters. dN^* has to be corrected for diffusion losses and magnification efficiency in the A11 nCNC system, k, and for the penetration efficiency of the sampling line, P.

$$\frac{dN^*}{dlogD_{P,i}} = \frac{dN^*}{logD_{50,i+1} - logD_{50,i}} \qquad \text{(Equation 2)}$$

were

$$dN^* = \left|TPNC\left(D_{50,i+1}\right) - TPNC\left(D_{50,i}\right)\right| \cdot \frac{k}{P} \qquad \text{(Equation 3)}$$

and

$$D_{P,i} = \sqrt[2]{D_{50,i+1} \cdot D_{50,i}} \qquad \text{(Equation 4)}$$

Table S2: Manufacturer specified k-factor for diffusion loss and magnification efficiency correction in the A11 nCNC. Penetration efficiency of sampling line following Gormley and Kennedy (1949) for a 0.6 m sampling line and 2.5 L/min flowrate.

$D_{P,i}$ [nm]	k-factor	Penetration efficiency, P
1.46	1.667	0.554
1.52	1.429	0.573
1.62	1.250	0.602
1.78	1.163	0.642
2.61	1.173	0.771
2.86	1.173	0.795

Table S3: Description of variables

Variable	Description	Unit
N	Total particle number concentration (TPNC)	$1/cm^3$
N^*	Corrected TPNC	$1/cm^3$
$D_{P,\,i}$	Midpoint particle diameter	nm
$D_{50,\,i}$	Lower 50% cut-off diameter	nm
$D_{50,\,i+1}$	Adjacent upper 50% cut-off diameter	nm

Investigation of the temperature setting of the Nano Enhancer

The temperature setting of the TSI 3757 Nano Enhancer was varied until the onset of homogenous nucleation, i.e., particle formation by the working fluid DEG, was observable. For this experiment, the Nano Enhancer was sampling HEPA-filtered room air and different saturator (T_S) and condenser (T_C) temperature settings were tested. While T_C was kept constant at 10°C, 11°C or 12°C, T_S was continuously increased over time and hold for about 3 – 5 minutes. A stabilization of the set T_S is typically achieved within 1 minute. Figure S1 shows that the number concentration was significantly increased above background when the temperatures T_C = 10°C/T_S = 66°C, T_C = 11°C/T_S = 67°C or T_C = 12°C/T_S = 68°C, were exceeded. To ensure that no homogenous nucleation occurs, we decided to conservatively add a safety buffer of 2°C. We therefore set the TSI 3757 Nano Enhancer setting at T_C = 12°C / T_S = 66°C / Δt = 54°C as high temperature mode (H).

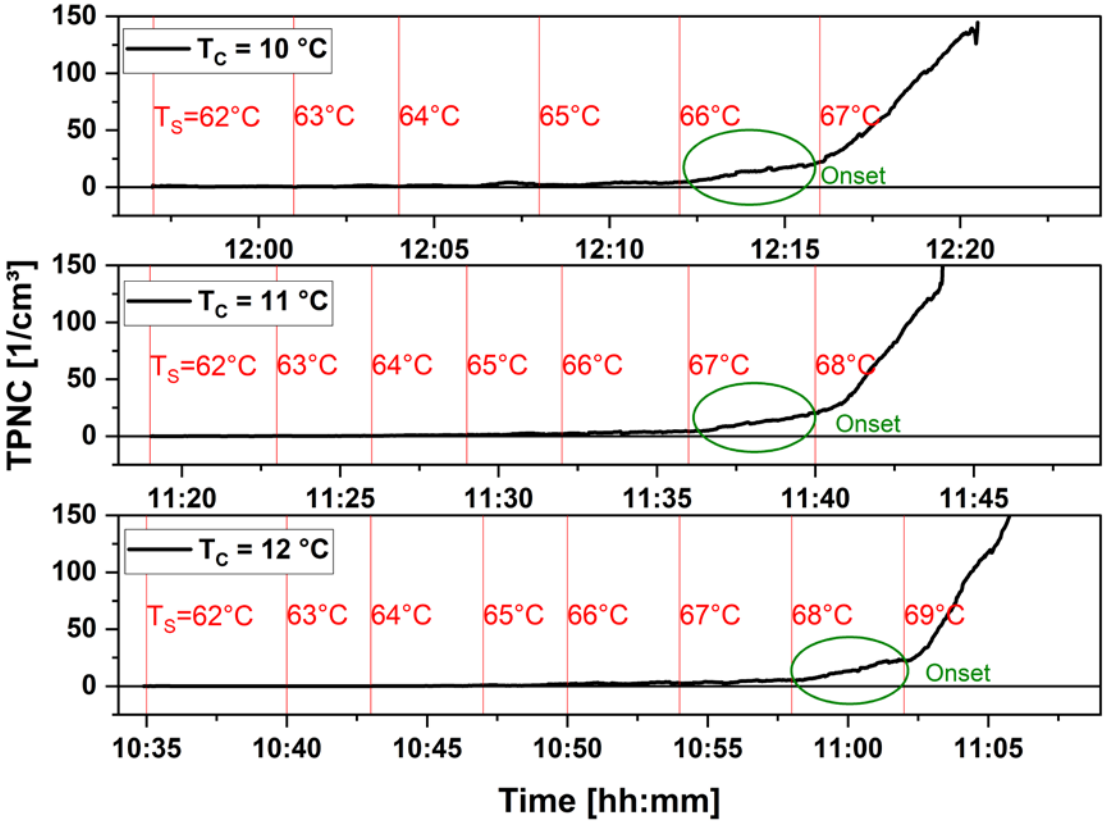

Figure S1: Boosting the temperature setting of the TSI 3757 Nano Enhancer. The black line depicts the smoothed TPNC moving average (1 min). The saturator temperature (T_S) was altered over time until the onset of homogeneous nucleation, indicated as significant increase in TPNC above background, occurs (marked with green ellipses). The condenser temperature (T_C) was kept constant at 10°C, 11°C or 12°C, respectively.

Instrumental set ups

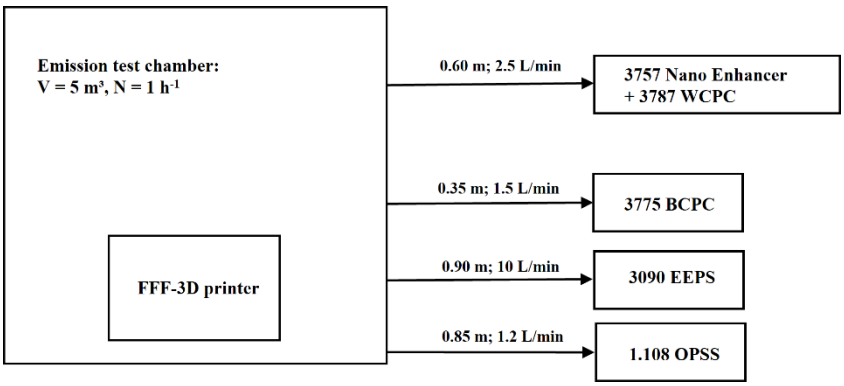

Figure S2: Schematic diagram of the instrumental set-up of the second experiment

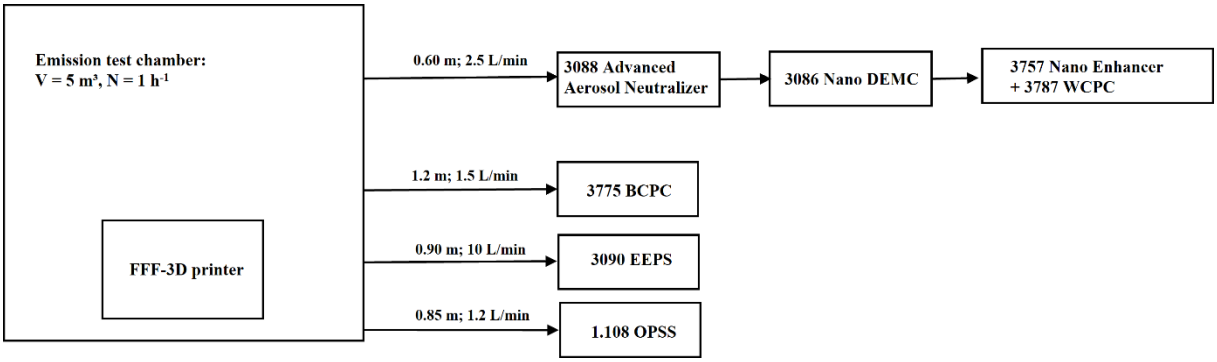

Figure S3: Schematic diagram of the instrumental set-up of the fourth experiment

Calibration of the 1 nm CPC

The detection efficiency of the 1 nm CPC was measured with a standard and high temperature setting using monodisperse NaCl particles as test aerosol (Merck AG, Germany) and a calibrated Faraday Cup Aerosol Electrometer (FCAE, BAM inhouse development) as a reference particle counter. Dry nitrogen was used as a carrier gas and the aerosol was generated in a three-zone tube furnace (GeRo GmbH, Germany). A porcelain crucible was filled with approximately 10 g of pro analysis grade NaCl and positioned in the third zone (last zone upstream of the furnace's exit). The third zone was actively heated and kept constant at 580 or 600°C (experiments on two days). Due to heat transfer the temperature in the first and the second zone also increased over time but did not exceed 270°C. Evaporation of NaCl occurred in the third zone and particles were formed downstream by rapid cooling to room temperature. The aerosol passed a TSI 3088 Advanced Aerosol Neutralizer and monodisperse fractions were generated with a TSI 3086 Nano Differential Electrical Mobility Classifier (Nano-DEMC) in classifier mode (i.e. at constant voltage). The aerosol flow through the Nano-DEMC may not exceed 2.5 L/min and hence was not sufficient to provide for both instruments, FCAE and CPC, under test with equal portions of the monodisperse test aerosol as described in ISO 27891:2015-03. Measurements with the 1 nm CPC and the FCAE were instead performed consecutively for selected particle sizes respectively over periods of several minutes and measurements of HEPA-filtered air in between to compensate the FCAE background. In total, five rounds were measured for each selected particle size and the arithmetic means $\bar{N}$ were calculated. The detection efficiency η for each of the sizes was determined using equation 5. The calibration setup is shown in Figure S4.

$$\bar{\eta} = \frac{\bar{N}_{1\ nm\ CPC}}{\bar{N}_{FCAE}} \qquad \text{(Equation 5)}$$

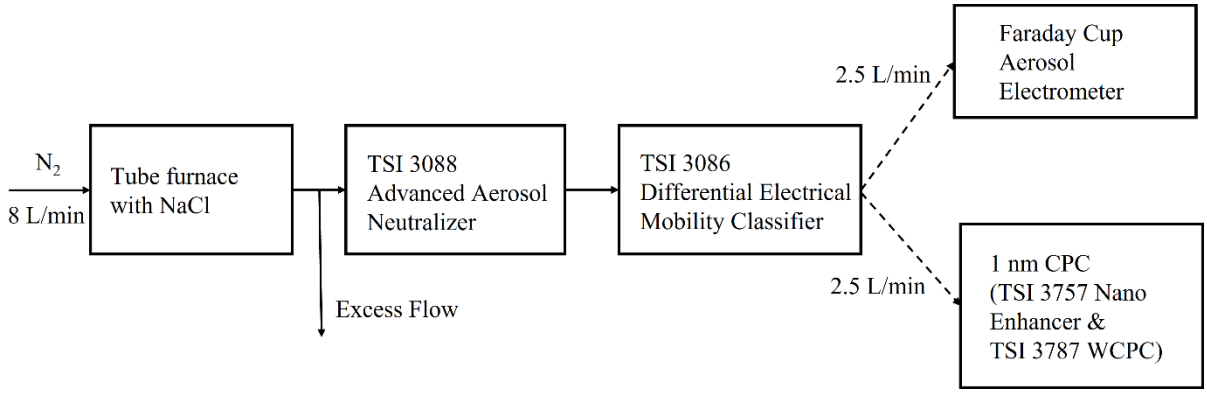

Figure S4: Calibration set-up with consecutive measurements in the FCAE- and the CPC branch

Ratio of 3775 BPC to 1nm CPC (S) concentrations during FFF-3D printing

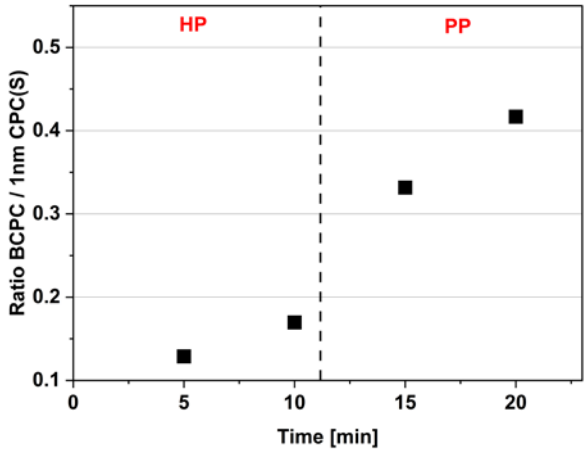

Figure S5: Ratio of BCPC to 1nm CPC(S) arithmetic mean concentrations during FFF-3D printing at the 5th, 10th, 15th and 20th minute.

Particle Size Spectra

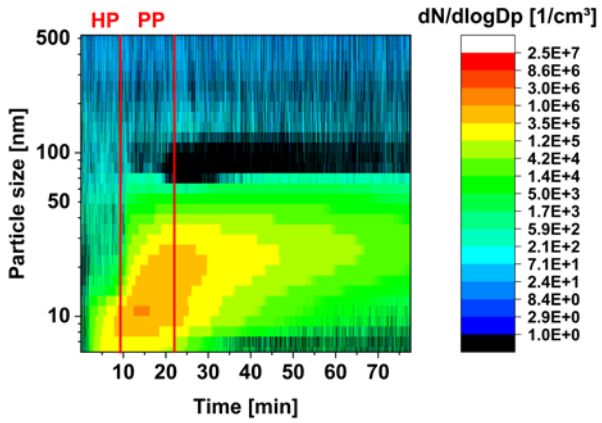

Figure S6: Normalized EEPS™ PNSD of the filament ABS-PR-01 printed on AnyM. Heating phase (HP) and printing phase (PP) are marked.

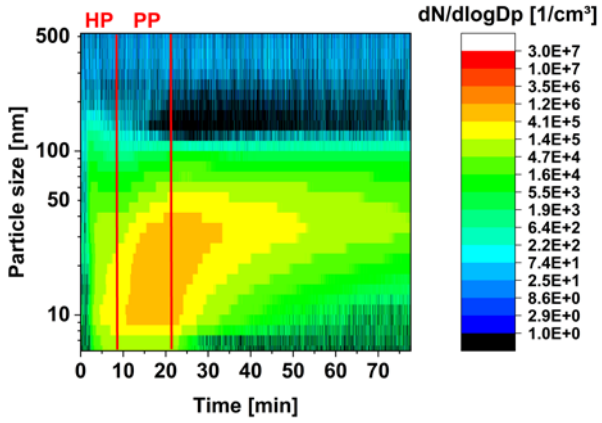

Figure S7: Normalized EEPS™ PNSD of the filament PEI-N-01 printed on CP(H-S). Heating phase (HP) and printing phase (PP) are marked.

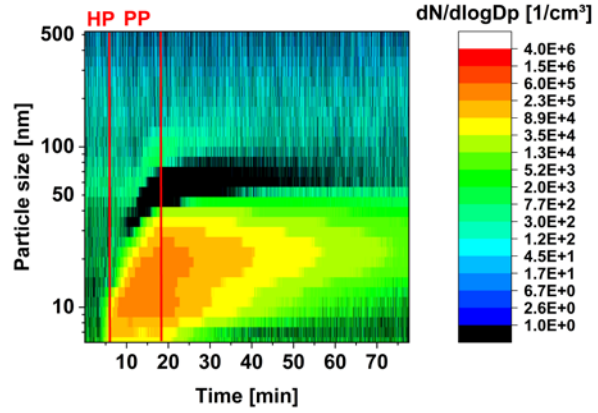

Figure S8: Normalized EEPS™ PNSD of the filament nGen-S -01 printed on CB2. Heating phase (HP) and printing phase (PP) are marked.

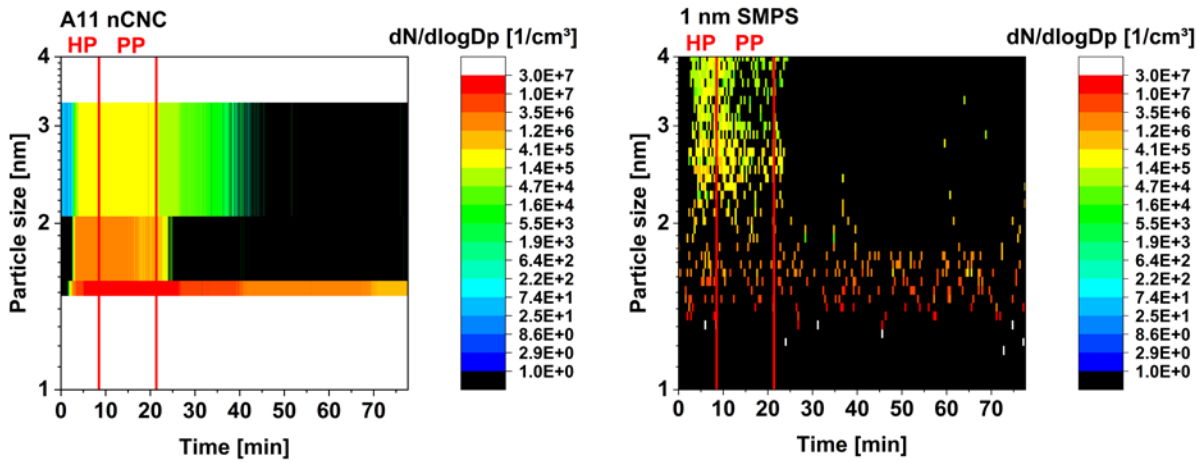

Figure S9: Normalized PNSD of the filament PEI-N-01 printed on CP(H-S). The A11 nCNC spectrum was compiled with four distinct D_{50} (1.5, 1.55, 1.7, 4 nm) measurements. The 1 nm SMPS scanned in the size range between 1 and 7 nm at 10 s time resolution. The sub-4nm section is displayed. Heating (HP) and printing phase (PP) are marked.

Evaluation and correction of diffusion loss in the sampling line

It can be expected that diffusional particle loss in sampling line will occur especially for particles in the sub-4 nm range. While the diffusion loss in the instrument is typically corrected by the manufacturer's software, diffusion loss prior entering the instrument inlet has to be evaluated. In this study, we used the Gormley and Kennedy (1949) laminar flow model to determine the diffusion loss. Figure S10 depicts the calculated particle penetration efficiency at laminar flow as a function of particle size, sampling flow rate and sampling line length. No diffusion loss occurs when the particle penetration efficiency is at 1. All size resolved data for the comparison in experiment 4 were corrected according to this model.

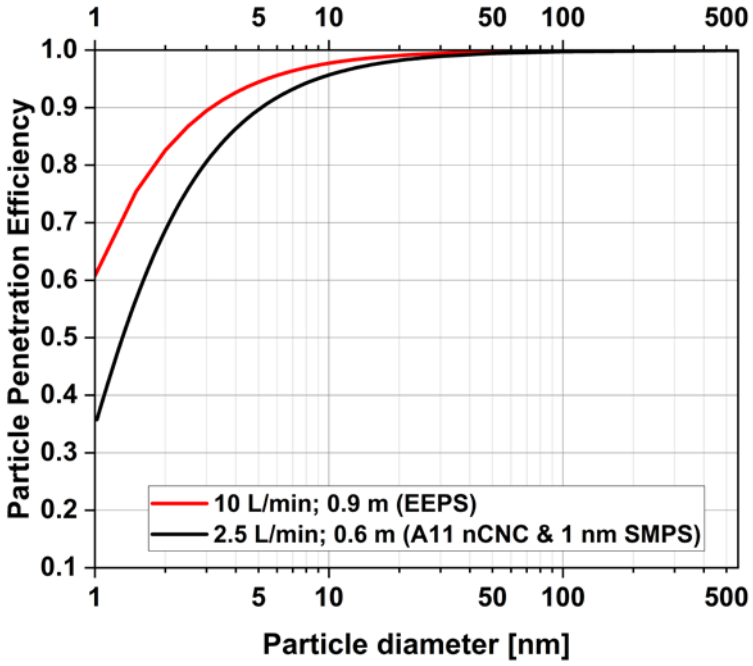

Figure S10: Particle penetration at laminar flow as a function of the particle size, sampling flow rate and sampling line length according to Gormley and Kennedy (1949) at T = 296 K, p = 101.3 kPa

In experiment 3, we compared the performance of the A11 nCNC (fixed mode) and the 1 nm CPC (S) as a particle counter. Due to lack of space, the arrangement of the instruments was limited at that time and hence the sampling line length differed between the A11 nCNC (0.6 m) and the 1 nm CPC (1.09 m) which might cause difference in sampling loss. Since only the TPNC is measured, size information is missing to apply the correction approach described above. Therefore, we compared the TPNC differences between the two sampling lines (0.6 and 1.09 m) in order to evaluate the losses relatively. As can be seen in Figure S11, the shorter sampling line showed no difference for the ABS-PR-01 filament considering the measurement uncertainty and only a slightly higher TPNC increase of 6.8 % ± 2.6 % at the end of printing for the PEI-N-01 filament. Since the effect is rather small, in a simplified manner the TPNC data of both instruments can be relatively compared with each other without diffusional loss correction for the sampling line.

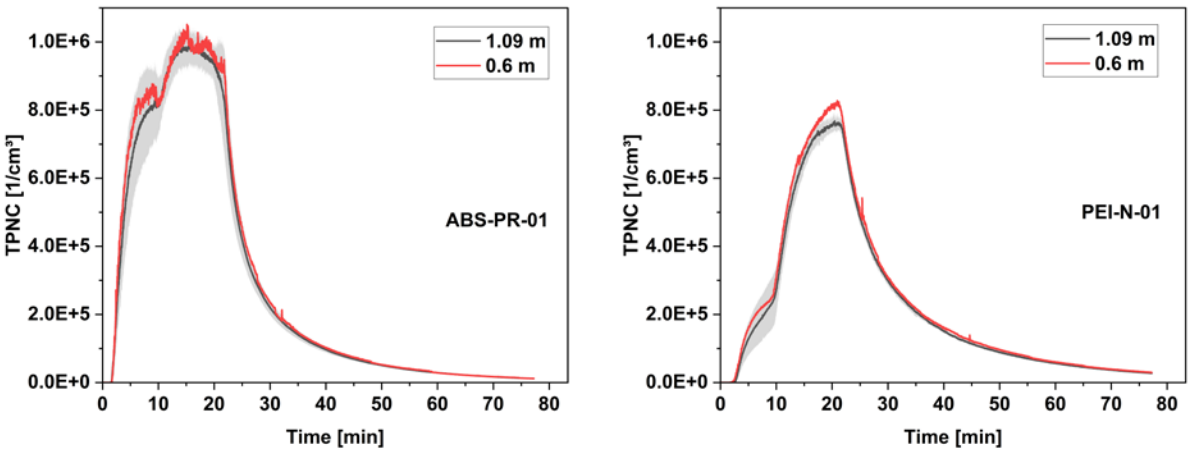

Figure S11: Evaluation of the diffusion losses from two different sampling line length. The TPNC during the 3D printing of two filaments were measured with the 1 nm CPC (S). The black line depicts the mean TPNC and the shaded area the standard deviation from repeat measurements (n=8 for ABS-PR-01, n=6 for PEI-N-01) for a 1.09 m long sampling line. The red line depicts the mean TPNC from two measurements for the shorter sampling line (0.6 m).

References

Gormley, P. G. and M. Kennedy. 1949. Diffusion from a stream flowing through a cylindrical tube. *Proceedings of the Royal Irish Academy. Section A: Mathematical and Physical Sciences* 52:163-169.